

# Strongly interacting Luttinger-liquid state in the integrable model of spinless fermions

Igor N. Karnaukhov

*Institute of Metal Physics, Vernadsky Street 36, 03142 Kiev, Ukraine*

(Received 14 August 2000; revised manuscript received 3 October 2000; published 3 January 2001)

A family of spinless fermion models with a hard core potential is formulated and solved by the Bethe ansatz method in one dimension for an arbitrary core radius. The Hamiltonian has two levels of strong interaction: the repulsive hard core potential and the kinetic energy with hopping integrals, values of which depend on the configuration of the particles. The Fermi velocity and the critical exponents describing the asymptotic behavior of the correlation functions at long distances have been calculated numerically for an arbitrary density of electrons and hard core radius. We discuss the effect of the hard core potential. The hard core potential defines an anomalous behavior of the critical exponent  $\Theta$  of the momentum distribution function. In the high-electron-density region the long-distance behavior is described by a strongly interacting Luttinger-liquid state with  $\Theta > 1$  and the residual Fermi surface disappears.

DOI: 10.1103/PhysRevB.63.045102

PACS number(s): 71.10.Fd, 71.10.Pm

Many one-dimensional quantum systems, in particular, interacting electron and spin systems, can be described as Luttinger liquids. In one-dimensional (1D) interacting systems all low-energy excitations are collective modes, whereas no quasiparticle type elementary excitations exist. Correlation functions then have nonuniversal, power-law behavior at low energies. The difficult feature inherent in the marginal liquid is the absence of a jump in the momentum distribution at the Fermi level  $k_F$ . Notably, it has been found that many integrable models, such as the 1D Hubbard model,<sup>1</sup> the supersymmetric  $t$ - $J$  model,<sup>2</sup> models with correlated hopping,<sup>3</sup> and models with long-range interactions,<sup>4</sup> exhibit different physical behavior. Different forms of the interaction have been studied in these models: on-site Coulomb repulsion, spin exchange coupling, and kinetic energy with correlated hopping.<sup>5</sup>

The aim of this article is to study the competition between, on the one hand, the kinetic energy with different hopping integrals and, on the other hand, the hard core potential with an arbitrary core radius. We argue that apart from the on-site Coulomb repulsion the hard core potential should be taken into account for description of the behavior of electrons in metals. The metallic properties of correlated 1D systems are not those of the usual Fermi liquid, but of the marginal liquid. We switch on the hard core potential in the integrable model of spinless fermions proposed recently in Ref. 6. The model Hamiltonian contains kinetic terms describing nearest-neighbor hopping with different hopping integrals, namely, the hopping integral  $t_n = t^{n-1}$  describes one-particle hopping in electron configurations with  $n$  particles. We investigate an extended version of the model<sup>6</sup> that is exactly soluble and exhibits a strongly interacting Luttinger-liquid behavior. This state is characterized by a large value of the critical exponent of the momentum distribution functions  $\Theta$  when the residual Fermi surface disappears. We show that a strongly interacting Luttinger-liquid state is formed at a high electron density as a result of strong correlations. The Hamiltonian of the modified model with the additional repulsion hard core interaction between electrons on a one-dimensional lattice with  $L$  sites and  $N$  electrons is given by

$$\mathcal{H} = - \sum_{i=1}^L (c_{i+1}^\dagger c_i + c_i^\dagger c_{i+1}) \sum_{n,m=0}^{\infty} t^{n+m} \mathcal{P}_{i,n}^- \mathcal{P}_{i+1,m}^+, \quad (1)$$

where  $c_i^\dagger$  and  $c_i$  are the creation and annihilation operators of electrons at site  $i$  and many-particle electron configurations are described via the  $\mathcal{P}$  operators  $\mathcal{P}_{i,n}^\pm = \prod_{r=1}^{\Delta+1} (1 - n_{i \pm n(\Delta+1) \pm r}) \prod_{\alpha=1}^n m_{i \pm \alpha(\Delta+1)}$  for  $n > 0$  and  $\mathcal{P}_{i,0}^\pm = \prod_{r=1}^{\Delta+1} (1 - n_{i \pm r})$  for  $n = 0$ . Here  $m_i = n_i \prod_{r=1}^{\Delta} (1 - n_{i+r})$  for  $\Delta > 0$  and  $m_i = n_i$  for  $\Delta = 0$ . The hard core interaction in Eq. (1) forbids two particles at distances smaller or equal to  $\Delta$  ( $\Delta = 0, 1, 2, \dots$  is measured in units of the lattice spacing parameter). By  $n_i = c_i^\dagger c_i$ , we denote the number operator for conduction electrons on site  $i$ , the hopping matrix element equal to unity for individual electrons. The case  $t = 1$  corresponds to hopping integrals of unity for an arbitrary electron configuration; as a result, the interaction terms in the model Hamiltonian (1) take into account the hard core potential of electrons only. A similar situation is realized for the case  $t = -1$ , since the contribution of the correlated hopping terms is an even function of the hopping integrals.

We write out the terms of the Hamiltonian (1) for  $\Delta > 0$  that illustrate the structure of the interaction for two- and three-particle complexes (see Fig. 1): for  $n = 2$ ,

$$\begin{aligned} \mathcal{H} = & -t \sum_{i=1}^L (c_{i+1}^\dagger c_i + c_i^\dagger c_{i+1}) \prod_{r=1}^{\Delta+1} (1 - n_{i-1-\Delta+r}) n_{i-1-\Delta} \\ & \times \prod_{r=1}^{\Delta} (1 - n_{i-1-\Delta+r}) \prod_{r=1}^{\Delta+1} (1 - n_{i+1+r}) \\ & -t \sum_{i=1}^L (c_{i+1}^\dagger c_i + c_i^\dagger c_{i+1}) \prod_{r=1}^{\Delta+1} (1 - n_{i-r}) \\ & \times \prod_{r=1}^{\Delta} (1 - n_{i+1+r}) n_{i+2+\Delta} \prod_{r=1}^{\Delta+1} (1 - n_{i+2+\Delta+r}), \end{aligned}$$

and for  $n = 3$ ,

$$\begin{aligned}
 \mathcal{H} = & -t^2 \sum_{i=1}^L (c_{i+1}^\dagger c_i + c_i^\dagger c_{i+1}) \prod_{r=1}^{\Delta+1} (1 - n_{i-2-2\Delta-r}) n_{i-2-2\Delta} \prod_{r=1}^{\Delta} (1 - n_{i-1-\Delta-r}) n_{i-1-\Delta} \\
 & \times \prod_{r=1}^{\Delta} (1 - n_{i-1-\Delta+r}) \prod_{r=1}^{\Delta+1} (1 - n_{i+1+r}) \\
 & -t^2 \sum_{i=1}^L (c_{i+1}^\dagger c_i + c_i^\dagger c_{i+1}) \prod_{r=1}^{\Delta+1} (1 - n_{i-r}) \prod_{r=1}^{\Delta} (1 - n_{i+1+r}) n_{i+2+\Delta} \prod_{r=1}^{\Delta} (1 - n_{i+2+\Delta+r}) n_{i+3+2\Delta} \prod_{r=1}^{\Delta+1} (1 - n_{i+3+2\Delta+r}) \\
 & -t^2 \sum_{i=1}^L (c_{i+1}^\dagger c_i + c_i^\dagger c_{i+1}) \prod_{r=1}^{\Delta+1} (1 - n_{i-1-\Delta-r}) n_{i-1-\Delta} \prod_{r=1}^{\Delta} (1 - n_{i-r}) \prod_{r=1}^{\Delta} (1 - n_{i+2+\Delta-r}) \\
 & \times n_{i+2+\Delta} \prod_{r=1}^{\Delta+1} (1 - n_{i+2+\Delta+r}).
 \end{aligned}$$

Two lines of the formulas for  $n=2$  and  $n=3$  correspond to one line in Figs. 1(a) and 1(b), respectively. Similar terms of the Hamiltonian (1) are represented in Ref. 6 for  $\Delta=0$ .

A detailed investigation of the integrability of model (1) for the case  $\Delta=0$  was presented in Ref. 6. The two-particle scattering matrix is multiplied by an additional scattering phase shift due to the hard core potential and the procedure

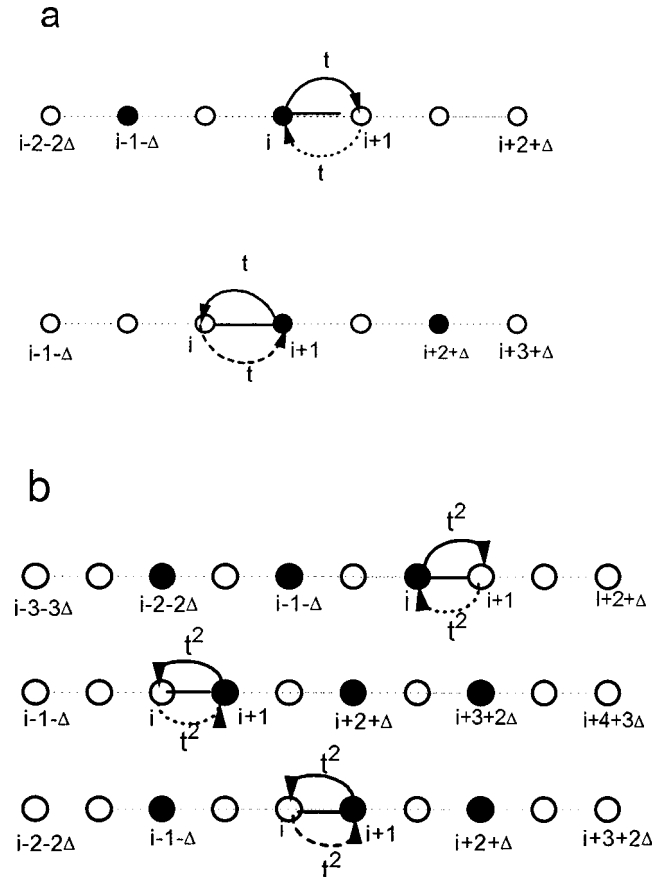


FIG. 1. Graphical representation of one-particle hopping in the configurations with two (a) and three (b) particles. The hopping matrix elements are equal to  $t$  for  $n=2$  and  $t^2$  for  $n=3$ .

for diagonalization of the Hamiltonian (1) is identical to that for the case  $\Delta=0$ . We now turn to discrete Bethe equations that generalize the ones for arbitrary  $\Delta$ . The quasimomenta are determined by the Bethe ansatz equations

$$\begin{aligned}
 \exp(ik_j L) = & (-1)^N \prod_{i=1}^N \exp \left[ i(k_j - k_i)(\Delta + 1) \right. \\
 & \left. - 2i\Theta \left( \frac{k_j - k_i}{2} \right) \right], \quad (2)
 \end{aligned}$$

where  $\Theta(\lambda) = \arctan(\coth \nu \tan \lambda)$ ,  $\tanh \nu = c$  for  $|c| < 1$ ,  $\Theta(\lambda) = \arctan(\tanh \nu \tan \lambda)$ , and  $\coth \nu = c$  for  $c > 1$ . The solution (2) is incorporated in the parameter  $c = 2/t^2 - 1$  varying in the intervals  $-1 < c < 0$ ,  $0 \leq c < \infty$ .

The total energy of the system in a state corresponding to solutions of  $\{k_j\}$  is

$$E = -2 \sum_{j=1}^N \cos k_j. \quad (3)$$

At  $\Delta=0$  the Bethe equations (2) are reduced to those for the model proposed in Ref. 6. We will briefly analyze the effect of the repulsive hard core potential for different values of the core radius. The results of the calculations are compared with those for  $\Delta=0$ . In the thermodynamic limit the quasimomenta  $\{k_j\}$  have, in general, complex values  $k_{j,p,n} = \lambda_{j,p} + i\mu(p-2n+1)/2$ ,  $n=1,2,\dots,p$ . The ground state of the system is described by real rapidities  $k_{j,1,1} = \lambda_{j,1}$  for the case of the repulsive effective interaction  $c > 0$  ( $|t| < \sqrt{2}$ ) and complex  $k_j$  (or strings with the length  $p$ , where  $p \rightarrow \infty$ ) for the attractive effective interaction  $c < 0$  ( $|t| > \sqrt{2}$ ).<sup>6</sup> The strings with  $p$  length describe the  $p$ -particle bound states; as a result, for  $c < 0$  the electrons form a cluster with  $N$  particles, in other words, a phase separation takes place. Let us analyze the  $c > 0$  case. In the thermodynamic limit the quasimomenta are closely spaced and may be regarded as a continuous variable. It is then usual to define the distribution function  $\rho(\lambda)$  for the set of quasimomenta. Taking loga-

rithms of Eq. (2), and afterwards performing the thermodynamic limit, we are able to obtain an integral equation of Fredholm's type for the distribution function  $\rho(\lambda)$  for the variable  $\lambda$ :

$$\rho(\lambda) - \int_{-Q}^Q d\lambda' R(\lambda - \lambda') \rho(\lambda') = \frac{1}{2\pi} [1 - (\Delta + 1)n], \quad (4)$$

with the kernel being

$$R(\lambda) = \frac{1}{2\pi} \frac{\sinh(2\mu)}{\cosh(2\mu) \mp \cos(\lambda)},$$

where the upper and lower signs correspond to the cases  $0 < c < 1$  ( $1 < |t| < \sqrt{2}$ ) and  $c > 1$  ( $|t| < 1$ ), respectively. The cutoff parameter  $Q$  is determined by the density of electrons; one finds  $n = \int_{-Q}^Q d\lambda \rho(\lambda)$ . The band filling is controlled by the parameter  $Q$ ;  $Q = \pi$  corresponds to a full band with density  $n_{max} = 1/(1 + \Delta)$ , while at  $Q = 0$  the band is empty. The solution of this equation yields the ground state energy per site:

$$\varepsilon = -2 \int_{-Q}^Q d\lambda \cos \lambda \rho(\lambda). \quad (5)$$

Below, we consider the behavior of electrons for several values of  $t$  and  $\Delta$  and an arbitrary electron density. We compare the results obtained for small ( $|t| < 1$ ) and large ( $1 < |t| < \sqrt{2}$ ) hopping integrals. Let us consider the Fermi velocity of electrons and the long-distance behavior of the correlation functions characterized by the critical exponents. The analysis of low-lying excitations shows that there is one massless branch of charge excitations. The Fermi velocity of the gapless charge excitation  $v = \varepsilon'(Q)/[2\pi\rho(Q)]$  (here by the prime we mean a derivative) is determined by the dressed energy  $\varepsilon(Q)$ , where  $\varepsilon(\lambda)$  is the solution of the integral equation

$$\varepsilon(\lambda) = -2 \cos \lambda - \mu + \int_{-Q}^Q d\lambda' R(\lambda - \lambda') \varepsilon(\lambda'), \quad (6)$$

such that  $\varepsilon(\pm Q) = 0$  ( $\mu$  is the chemical potential).

In Fig. 2 we show the Fermi velocity calculated numerically for two values of  $t$  ( $t = 0.5$  or  $c = 7$  and  $t = 1.3$  or  $c = 0.183$ ) and  $\Delta = 0, 1, 2, 3$ . We see that the Fermi velocity decays to zero at the extreme densities  $n \rightarrow 0$  and  $n \rightarrow n_{max}$ . The system is metallic except at the extreme electron concentrations. It is to be noted that at  $n_{max}$  the model displays a metal-insulator phase transition in the insulator phase with a new spacing parameter  $\Delta + 1$ . We clearly observe a different behavior of  $v$  for  $|t| < 1$  and  $1 < |t| < \sqrt{2}$ . This is easily understood: the fermions are more mobile in small complexes at  $|t| < 1$  and in large complexes at  $1 < |t| < \sqrt{2}$ . The height of the maximum is shifted in the small-electron-density region at  $|t| < 1$  and in the high-electron-density region at  $1 < |t| < \sqrt{2}$ . For  $|t| = 1$  the maximum of the Fermi velocity is realized at a "half-filling" density  $1/(2 + \Delta)$ . The maximal value of  $v$  increases with  $\Delta$ .

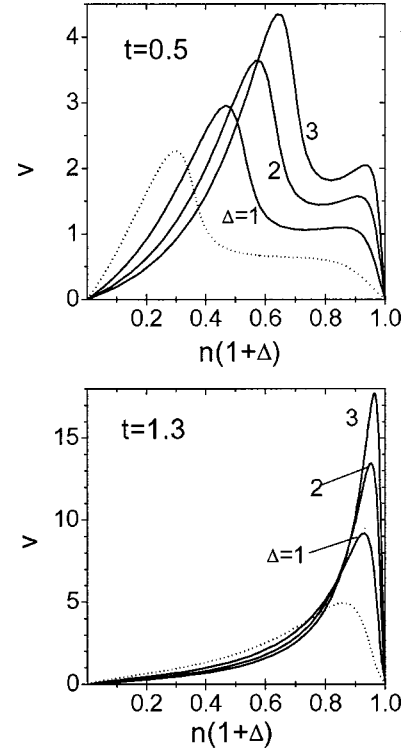


FIG. 2. The Fermi velocity versus the electron density. The individual curves are labeled by the value of the parameter  $\Delta$ . The result for  $\Delta = 0$  is plotted (dotted line) for comparison.

The long-distance behavior of the density-density correlation function is given by

$$\langle n(x)n(0) \rangle \approx n^2 + A_1 x^{-2} + A_2 x^{-\alpha} \cos(2k_F x), \quad (7)$$

where  $n(x_i) = n_i$ ,  $k_F$  is the Fermi momentum, and  $\alpha = 2[\xi(Q)]^2$ .  $\xi(Q)$  is the dressed charge at the Fermi surface; the dressed charge function  $\xi(\lambda)$  is defined as  $\xi(\lambda) = 2\pi\rho(\lambda)$ .

The exponent  $\alpha$  is plotted in Fig. 3. In the low-density limit  $n \rightarrow 0$  and, as for  $|t| \rightarrow 1$ , the value of  $\alpha \rightarrow 2$ , which is the same as for noninteracting fermions. This value separates the regimes with dominant correlation effects in the density-density correlation function. The oscillating term in Eq. (7) dominates in the high-density region for large hopping integrals at an arbitrary electron core radius. The value of  $\alpha$  decreases with  $\Delta$  and, as a result, the region with dominant correlations grows. Similar behavior of  $\alpha$  is observed for small hopping integrals at  $\Delta > 0$ .

Let us compare the asymptotic behavior of the density-density correlation function (7) with that of the pair correlation function

$$\langle C^\dagger(x)C(0) \rangle \approx A_3 x^{-\beta}, \quad (8)$$

where  $C^\dagger(x_i) = c_i^\dagger c_{i+1}^\dagger$  and the critical exponent  $\beta$  is given by the inverse of  $\alpha$  ( $\beta = 1/\alpha$ ). In Fig. 3 we indicate (dashed line) the region with dominant pair correlations when  $\alpha > 1$ . The range of this region depends on the hopping integral and the core radius. An analogous behavior of the correlation functions is observed in models with attractive effective in-

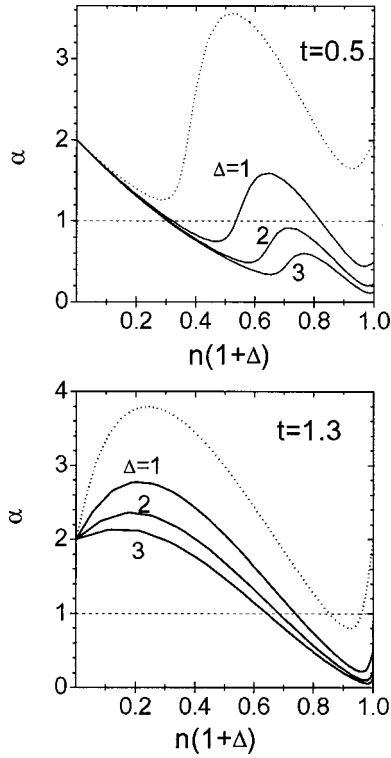


FIG. 3. The exponent  $\alpha$ . As in Fig. 2 for values of  $\alpha$  above the dashed line we have dominant pair correlations.

teraction of the particles when the ground state configuration contains a bound pair characterized by a pair of complex particle rapidities with a finite binding energy.<sup>7</sup> In the supersymmetric  $t$ - $J$  model the spin and charge rapidities are classified as bound states with an arbitrarily small binding energy; therefore this system does not manifest superconducting properties. In contrast with other models<sup>7</sup> the regions with dominant pair correlations is realized on the basis of the real rapidities of the Bethe ansatz equations. In regions with dominant density-density correlations the particles prefer to move individually, instead of by pair hopping, but in the region with pair correlations they create two-atom molecules. As we will see below, at high electron density the repulsive hard core potential stimulates formation of a strongly interacting Luttinger-liquid state, destroying the pair correlations.

The correlation effects produced by the hard core potential are most impressively displayed in the momentum distribution function. The momentum distribution function around the Fermi point can be written as

$$\langle n_k \rangle \approx \langle n_{k_F} \rangle - \text{const} \times |k - k_F|^\Theta \text{sgn}(k - k_F), \quad (9)$$

where the exponent  $\Theta$  is expressed in terms of  $\alpha$ ,

$$\Theta = \frac{1}{\alpha} \left( 1 - \frac{\alpha}{2} \right)^2. \quad (10)$$

In Fig. 4 the correlation exponent  $\Theta$  is shown as a function of the electron density for the same values of the hard core radius. For  $n=0$  we have the Fermi liquid result  $\Theta=0$ .

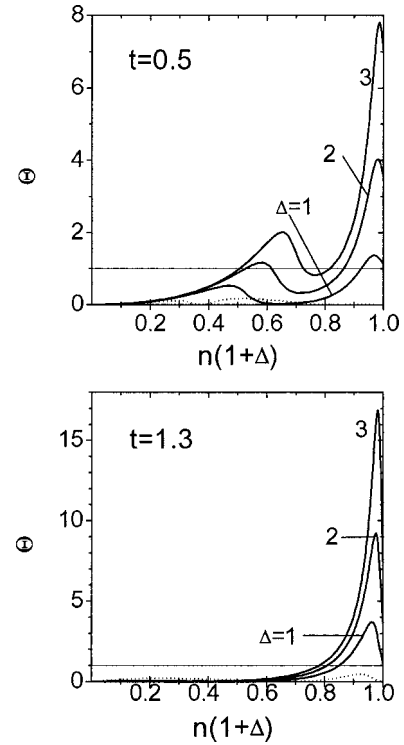


FIG. 4. The exponent  $\Theta$  as a function of the electron density for  $t=0.5$  and  $t=1.3$ . The solid line separates the strongly interacting Luttinger-liquid state.

Due to strong electron correlations the value of  $\alpha$  decreases with  $\Delta$  and consequently the value of  $\Theta$  increases.  $\Theta$  is a nonmonotonic function of the electron density; it has one maximum for  $1 < |t| < \sqrt{2}$  or two for  $|t| < 1$ . The maximum value of  $\Theta$  is realized in the high-electron-density region when the interaction between particles prevails; on the other hand, at a low electron density the distribution of the particles is so dilute as to render the effect of interaction negligible. In Fig. 4 we separate by the solid line the region of density that corresponds to a strongly interacting Luttinger-liquid state with  $\Theta > 1$ . For comparison we plot in Fig. 5 the results of calculations for  $\Theta$  at  $t=1$ . This is the case of a ‘‘pure’’ hard core interaction between particles.  $\Theta$  is an increasing function of the electron density for all  $\Delta > 0$ . The

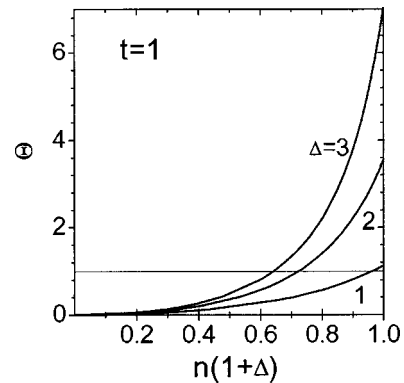


FIG. 5. The exponent  $\Theta$  as a function of the electron density for  $t=1$ .

resultant critical exponent  $\Theta=0$  is a canonical exponent characteristic of the noninteracting electron system (for  $\Delta=0$ ). We see that  $\Theta$  increases rapidly with increasing band filling in the high-density region, reaching the maximum value  $\frac{1}{2}[\Delta(\Delta+2)/(1+\Delta)]^2$  at the extreme concentration  $n_{max}$ . Comparing the behavior of  $\Theta$  in Figs. 4 and 5, we see that both the hard core potential and the correlated hopping give rise to a strongly interacting Luttinger-liquid state in the high-density region.

To summarize, we have introduced an integrable two-parameter model of spinless fermions on a discrete lattice. The exact solution allows for a detailed study of the asymptotic behavior of the correlation functions. Note the unusual properties of the model proposed. There are two distinct regimes of the phase diagram with dominating

density-density or pair correlations. In the low-density region where the hard core potential is of little consequence the pair correlations dominate. In the high-electron-density region where density-density correlations dominate the state is identified as a strong interacting Luttinger liquid with  $\Theta>1$ . This state is realized due to the strong interaction of the particles via correlated hopping and the hard core potential. In the high-density limit the model exhibits a metal-insulator transition in the insulator phase with the new spacing parameter  $\Delta+1$ .

The author would like to thank A. A. Ovchinnikov for many stimulating discussions. The author acknowledges the support of the Max-Planck-Institut für Physik Komplexer Systeme, Dresden, Germany, and of the International Centre for Theoretical Physics, Trieste, Italy.

<sup>1</sup>E.H. Lieb and F.Y. Wu, Phys. Rev. Lett. **20**, 1445 (1968).

<sup>2</sup>Bill Sutherland, Phys. Rev. B **12**, 3795 (1975); P. Schlottmann, *ibid.* **36**, 5177 (1987); P.A. Bares *et al.*, *ibid.* **44**, 130 (1991).

<sup>3</sup>I.N. Karnaukhov, Phys. Rev. Lett. **73**, 1130 (1994); F.C. Alcaraz and R.Z. Bariev, Phys. Rev. B **59**, 3373 (1999); F. Dolcini and A. Montorsi, cond-mat/9912321 (unpublished).

<sup>4</sup>F.D.M. Haldane, Phys. Rev. Lett. **60**, 365 (1988); B.S. Shastry, *ibid.* **60**, 639 (1988); A. Polychronakos, *ibid.* **70**, 2329 (1990); Bill Sutherland and B.S. Shastry, *ibid.* **71**, 5 (1993); M. Arikawa

*et al.*, cond-mat/9907139 (unpublished).

<sup>5</sup>V.E. Korepin and F.H.L. Essler, *Exactly Solvable Models of Strongly Correlated Electrons* (World Scientific, Singapore, 1994); V.E. Korepin, N.M. Bogolubov, and A.G. Izergin, *Quantum Inverse Scattering Method and Correlation Functions* (Cambridge University Press, Cambridge, 1993).

<sup>6</sup>I.N. Karnaukhov, Phys. Rev. B **60**, 15 496 (1999).

<sup>7</sup>R.Z. Bariev *et al.*, J. Phys. A **26**, 1249 (1993); I.N. Karnaukhov, Int. J. Mod. Phys. B **10**, 3673 (1996).